International Symposium on Cavitation, CAV'95, May 1995, Deauville, FRANCE

MODELS OF CAVITATION EVENT RATES

by

Zhenhuan LIU
Christopher E. BRENNEN
California Institute of Technology
PASADENA - USA

MODELS OF CAVITATION EVENT RATES

Zhenhuan Liu
Christopher E. Brennen

California Institute of Technology
Pasadena, California 91125
U.S.A.

ABSTRACT

To model the processes of cavitation inception, noise, and damage, it is necessary to generate a model of the cavitation event rate which can then be coupled with the consequences of the individual events to produce a complete synthesis of the phenomenon. In this paper we describe recent efforts to connect the observed event rates to the measured distributions of cavitation nuclei in the oncoming stream. A comparison is made between the observed event rates and event rates calculated from measured nuclei distributions using an algorithm which includes the dynamics of the nuclei motion and growth. Various complications are explored including the relative motion between the nucleus and the liquid, the effect of the finite bubble size of the growing bubble relative to the dimensions of the low pressure region, and the effect of bubble growth on neighboring nuclei. All of these are seen to have an important influence on the event rate, and therefore, on cavitation inception and other macroscopic consequences. We demonstrate that it is possible to predict the correct order of magnitude of the event rate when an attempt is made to model the important flow complications.

NOMENCLATURE

C	Nuclei concentration
C_P	Coefficient of pressure, $(p-p_\infty)/\frac{1}{2}\rho U^2$
C_{PM}	Minimum C_P on a given streamline
C_{PMS}	Minimum value of C_P on the headform surface
D	Headform diameter
E	Cavitation event rate
$N(R)$	Nuclei density distribution function
R	Radius of a cavitation nucleus
R_C	Critical cavitation nucleus radius
R_{max}	Maximum cavitation bubble radius
R_0	Initial nucleus radius
S	Surface tension
U	Upstream tunnel velocity
f_1, f_2, f_3	Numerical factors effecting the cavitation event rate
n_i	Bubble/bubble interaction effect
p	Fluid pressure
p_∞	Pressure upstream
p_{G0}	Initial gas pressure in a bubble
p_{min}	Undisturbed liquid pressure
p_v	Vapor pressure
p_c	Blake critical pressure
r	Distance from the center of a bubble
r_S	Radius of minimum pressure point
r_c	Critical radius
y	Normal off-body distance
y_M	Maximum normal off-body distance of the $C_P = -\sigma$ isobar
ρ	Fluid density
σ	Cavitation number, $(p_v - p_\infty)/\frac{1}{2}\rho U^2$

σ_i Inception cavitation number
σ_i' Cavitation number variation

1. INTRODUCTION

In order to synthesize the cumulative effects of a stream of traveling cavitation bubbles, it is necessary to supplement the details of individual events with the rates at which these events occur. Many investigators have anticipated a relationship between the cavitation event rate and the concentration of cavitation nuclei in the oncoming stream (see, for example, Schiebe [31], Keller [13][14], Keller and Weitendorf [15], Kuiper [16], Gates and Acosta [9], Meyer *et al.* [24]). At first sight this seems like a straightforward problem of computing the flux of nuclei into the region for which $C_P < -\sigma$. However many complications arise which make this analysis more complicated than might otherwise appear and we shall discuss some of the specific issues below. But these difficulties do not account for the lack of experimental research into the relationship. Rather, the difficulties involved in the accurate measurement of the incoming nuclei number distribution function, $N(R)$, have been responsible for the delay in any detailed, quantitative investigation of this component of the problem. (Note that $N(R)dR$ is the number of nuclei with size between R and $R + dR$ per unit volume). As Billet [3] remarked in his review of nuclei measurement techniques, the only reliable method of obtaining $N(R)$ has been the extremely time consuming procedure of surveying a reconstruction of an *in situ* hologram of a small volume of tunnel water. However, the time and effort required to construct one $N(R)$ distribution by this method has seriously limited the scope of these investigations.

The recent development of light scattering instruments employing phase Doppler techniques (Saffman *et al.* [30], Tanger *et al.* [32]) and of cavitation susceptibility devices (Oldenziel [25], and Le Goff and Lecoffre [19]) has improved the situation. In our own laboratory we have attempted to validate and calibrate a Dantec Phase Doppler Anemometer (PDA) instrument by taking simultaneous measurements with the PDA and a holographic system (Liu *et al.* [21]). The great advantage of the PDA system is the speed with which $N(R)$ can be measured. After validation, the PDA system could then be used with confidence for investigations of the nuclei population dynamics in a water tunnel (see Liu *et al.* [21]) and of the aforementioned relation between $N(R)$ and the cavitation event rate (Liu *et al.* [22], and Liu and Brennen [23]).

In this paper, we first present the experimental observations of cavitation event rates on a Schiebe headform with simultaneous measurement of the nuclei distribution in the upcoming stream. We then further refine the analytical model of Liu *et al.* [22], to synthesize the event rates from the measured nuclei distributions. Then we compare the predicted event rates with cavitation observations in two water tunnels with quite different nuclei population dynamics.

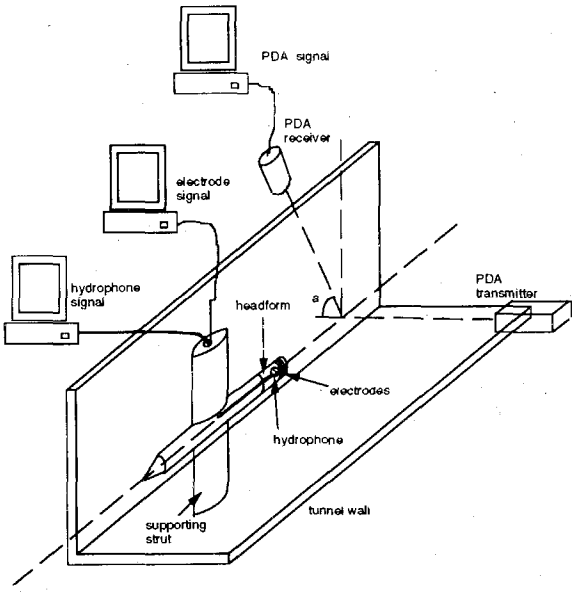

Figure 1: A sketch of the experimental setup. The upstream nuclei distribution is measured by a PDA and the cavitation event rate is measured by the surface electrodes.

2. EXPERIMENTS

The data presented in this paper was taken during tests conducted in the Low Turbulence Water Tunnel (LTWT) and the High Speed Water Tunnel (HSWT) at Caltech. An axisymmetric headform (Schiebe headform shape, Schiebe [31]) measuring $5.08cm$ in diameter was installed on the centerline of the tunnel, as shown in figure 1. Three flush ring electrodes of silver epoxy covering the entire periphery were installed in the lucite headform and allowed the detection of cavitation events occurring on the headform (Ceccio and Brennen [7]). A pattern of alternating voltages is applied to the electrodes, and the electric current from each is monitored. When a bubble passes over one of the electrodes, the impedance of the flow is altered causing a drop in current which can be detected. Thus, event statistics such as the event rate and event duration are readily accumulated.

A Phase Doppler Anemometer made by Dantec was used to simultaneously measure the fluid velocity and nuclei number distribution, $N(R)$, on the center line of the water tunnel, $16cm$ upstream of the Schiebe body. The PDA uses a $200mW$ Argon-ion laser with $514.5nm$ wavelength. The transmitting optics were mounted horizontally to project through a side window; the receiving optics were mounted above the top window and focused on the center plane of the water tunnel (See figure 1). The receiving optics collected light scattered at an angle of 82° to the incident laser beams. The resulting focal volume measured $0.204\,mm \times 0.203\,mm \times 2.348\,mm$.

3. OBSERVATIONS OF NUCLEI POPULATION AND EVENT RATES

In figure 2, we present a typical comparison of nuclei number density distributions in the LTWT and in the HSWT. Also plotted in the figure are measurements in

other facilities (Arndt [1], Peterson *et al.* [27][28], Feldberg and Shlemenson [8] and Gates and Bacon [10]) and in the ocean (Cartmill and Su [6]). Substantial differences in the nuclei number density distribution were found between the two tunnels. Although the shapes of the distributions are similar, the differences in the magnitude can be as much as two orders of magnitude. We note that the nuclei population in the LTWT is large while the population in the HSWT is small. The typical nuclei concentration in the LTWT is about $100cm^{-3}$; while the nuclei concentration in the HSWT is about $1cm^{-3}$. Billet [3] and Gindroz and Billet [11] presented useful reviews of the subject of nuclei concentrations and distributions. They found that for de-aerated water, typical concentrations are of the order of $20cm^{-3}$ with sizes ranging from about $5\mu m$ to about $200\mu m$. We conclude that the LTWT is nuclei rich and the HSWT is nuclei poor. Therefore, comparative experiments in the two tunnels should provide a valuable range of nuclei population effects.

Figure 3 presents the observations of event rates on a Schiebe headform in both the LTWT and HSWT experiments. As shown in these figures, the cavitation event rates increased dramatically as the cavitation number is decreased. However, the event rates can vary by as much as a decade at the same cavitation number. At the same cavitation number, larger free-stream nuclei concentrations correspond to larger cavitation event rates. As one would expect, the event rates observed at the same cavitation number in the LTWT are much higher than in the HSWT, because of the much higher nuclei population in the LTWT.

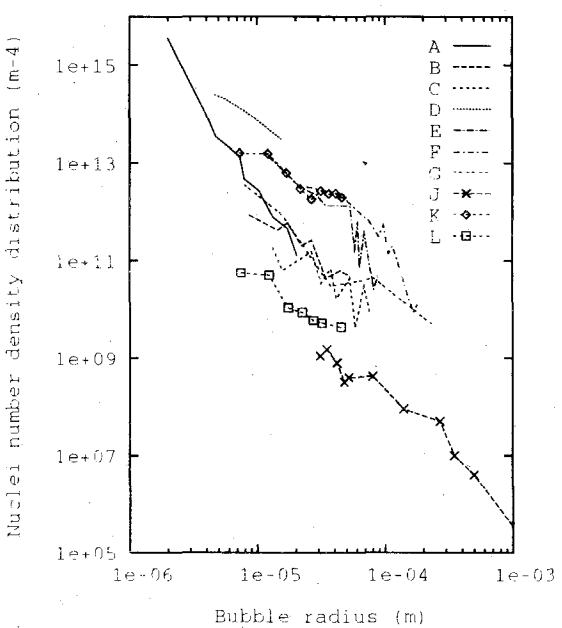

Figure 2: A comparison of the nuclei number density distributions in the Low Turbulence Water Tunnel and the High Speed Water Tunnel with measurements in other facilities and in ocean. (**A**): Peterson *et al.* [28], light scattering method, (**B**): Peterson *et al.* [28], holographic method, (**C**): Peterson *et al.* [27], (**D**): Feldberg and Schlemenson [8], (**E**): Arndt and Keller [1], (**F**): Keller and Weitendorf [15], (**G**): Gates and Bacon [10], (**J**): Cartmill and Su [6] , (**K**): current study, LTWT, (**L**): current study, HSWT.

During the tests in the HSWT, cavitation experiments were performed at various tunnel speeds and air contents. As shown on the right in figure 3, the nuclei population not only has an effect on the event rate but also has an effect on the cavitation inception number. For example, at a velocity of $9.4m/sec$ and a nuclei concentration of $0.8cm^{-3}$, the cavitation inception number was 0.47. After air injection, the nuclei concentration rose to $12cm^{-3}$, and cavitation inception occurred at $\sigma_i = 0.52$. It should be recalled that, in the LTWT, the cavitation inception number was about 0.57, and the nuclei concentration was about $100cm^{-3}$. In the HSWT, attached cavitation occurred soon after traveling bubble cavitation. This implies that attached cavitation occurs more readily when the nuclei population is low. Li and Ceccio [20] observed a similar phenomenon on a cavitating hydrofoil. In their observations, when the nuclei concentration in the water was high, traveling bubble cavitation occurred before attached cavitation was observed. But when the nuclei concentration was low, no traveling bubble cavitation was observed before attached cavitation occurred. They ascribe the cause of this phenomenon to laminar boundary separation on the hydrofoil. However, we are not sure about the cause on the Schiebe headform since it does not exhibit laminar boundary layer separation in the region of low pressure.

One should also note in the right of figure 3, by comparing the event rates at $U = 9.4m/sec$ and $U = 14.5m/sec$, that, at the same nuclei concentration level, $1.6cm^{-3} < C < 3.0cm^{-3}$, the cavitation event rate decreased with increasing tunnel velocity, which is the inverse of what would be expected. All the numerical and analytical simulations (Ceccio and Brennen [7], Meyer *et al.* [24], and Liu *et al.* [22]) predict that the event rate increases with oncoming velocity, provided that the nuclei population remains the same. This velocity effect on the cavitation event rate was also observed by Kuhn de Chizelle *et al.* [17][18]. Since they were unable to measure the nuclei population in the oncoming flow, Kuhn de Chizelle *et al.* speculated that the free nuclei population was decreased by the increase in tunnel pressure at a higher speed, but at the same cavitation number. The investigations of nuclei population dynamics in a water tunnel by Liu *et al.* [21] support their speculations. However, the current data shows that the event rates decrease with an increasing tunnel speed even when the nuclei concentrations are at the same level. This phenomenon is not fully understood. A possible explanation is that the PDA mistakenly counted more solid particles as microbubbles at the higher tunnel velocities. Since the population of solid particles increased with speed, perhaps the number of microbubbles population decreased even though the total nuclei concentration remained the same. It may also be the case that there exists some, as yet unrecognized, mechanism in the relation between the nuclei population and the cavitation event rate.

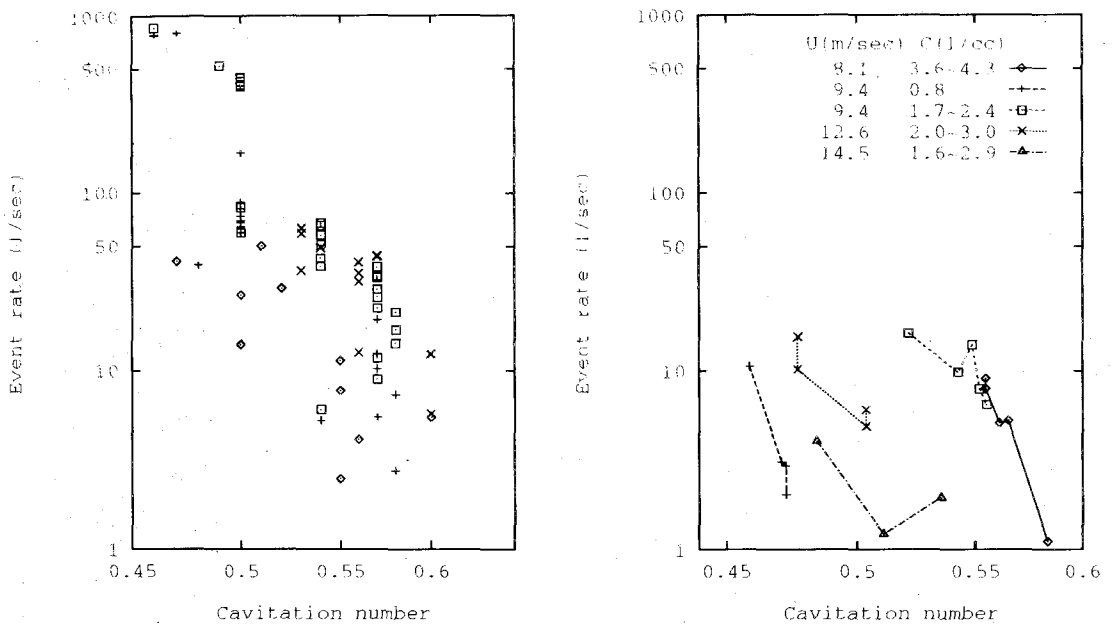

Figure 3: **Left**: Variations in the cavitation event rates with cavitation number on a 5.08cm Schiebe body in the LTWT at a speed of $9m/sec$. Data is plotted for various ranges of free stream nuclei concentration, C (cm^{-3}), as follows: $C < 150$ ($\diamond$); $150 < C < 200$ ($+$); $200 < C < 250$ ($\triangle$) and $250 < C$ ($\times$). **Right**: Observed cavitation event rates on a 5.08cm Schiebe body in the HSWT at various speeds and nuclei concentrations as indicated.

4. MODELS OF CAVITATION EVENT RATES

It has long been recognized that cavitation is caused by microbubbles being convected to the low pressure region. If the nuclei were to follow the fluid motion without any slip, and if the bubble was always spherical and always small relative to the important dimensions of the flow, the problem would be relatively simple. For each streamtube passing close to the body in which nuclei are likely to grow into macroscopic bubbles, one could input the pressure time history into the Rayleigh-Plesset equation and, for a range of initial nuclei sizes and cavitation numbers, calculate the resulting cavitation bubble size history. Such, of course, was the approach taken in the pioneering work of Plesset [29], Parkin [26] and others (see Brennen [5]). But there are other complications which occur in the actual flow and create more serious problems. First, the boundary layer on the headform surface will clearly have an effect on the volume flux through the low pressure region. Second, the relative motion between the nuclei and the liquid can be important. Johnson and Hsieh [12] included relative motion in their analysis and identified an important phenomenon which occurs when the nuclei experience the large fluid accelerations in the vicinity of the stagnation point. Specifically, the nuclei migrate outwards onto streamlines further from the stagnation streamline/body surface as a result of the large centripetal accelerations near the stagnation point. And the larger the nuclei, the larger this shift so that the flow acts as a screen or filter. The larger nuclei which are those most likely to cavitate may, in fact, be so displaced that they no longer experience tension in the low pressure region.

Other complications arise because the growing bubble rapidly reaches a size which is comparable to important dimensions such as the height above the headform surface, y_M, of the critical isobar, $C_P = -\sigma$. As a result, different parts of the bubble surface are exposed to different pressures and the bubble itself changes the local pressure distribution within the flow. Then it becomes necessary to resort to a complex procedure such as that of Kuhn de Chizelle *et al.* [17][18] in order to calculate the shape and growth of the bubble. Such analyses, which would take the place of the Rayleigh-Plesset calculations, are too complex for inclusion in the present event rate analyses, at least initially.

Liu *et al.* [22] presented an asymptotic approach to the connection between the event rate and the nuclei population, which included many of the above complications. They found that an event rate, E, given by

$$E = \int_0^{y_M f_3} 2\pi r_S U (1 - C_{PMS})^{\frac{1}{2}} f_1(y) \int_{R_C(y)}^{\infty} \frac{N(R)dR}{f_2(R,y)(1+n_i)} dy \qquad (1)$$

where f_1, f_2 and f_3 represent the boundary layer effect, the bubble screening effect and the finite bubble size effect, respectively (f_1, f_2 and f_3 are unity in the absence of these effects) and n_i denotes the effect of bubble/bubble interactions (see below). The critical nucleus radius, R_C, and the functions f_1, f_2 and f_3 were discussed in detail by Liu *et al.* [22] and that discussion will not be repeated here. Rather, we focus on refinement of the model to include the interactions between bubbles.

As a bubble grows in the low pressure region, the pressure field close to the bubble is altered. Within a certain distance close to the growing bubble the pressure pertur-

bation due to bubble growth increases the local pressure above the critical pressure at which a nuclei will cavitate. Thus, a nucleus in this volume will not cavitate. We will explore this bubble interaction effect in more detail.

To quantify the effect, we need to calculate the liquid volume in which the local pressure is larger than the Blake critical pressure, p_c, (Blake [4])

$$p_c = p_v - \frac{4S}{3}\left[\frac{2S}{3p_{G0}R_0^3}\right]^{\frac{1}{2}} \tag{2}$$

When a bubble is growing, the pressure perturbation in the surrounding liquid is given by

$$\frac{p(r) - p_{min}}{\rho} \approx \frac{R}{r}(R\ddot{R} + 2(\dot{R})^2) \tag{3}$$

where p_{min} is the undisturbed liquid pressure. When $R \gg R_0$, the pressure perturbation can be simplified using the Rayleigh-Plesset equation and written as

$$p(r) - p_{min} = \frac{4}{3}\frac{R}{r}(p_v - p_{min}) \tag{4}$$

For another nucleus to cavitate, the local pressure must be smaller than the Blake critical pressure. Solving for $p(r) < p_c$, we find the radius of the volume within which another nucleus will not cavitate:

$$r > \frac{4}{3}\frac{(-C_P - \sigma)}{(-C_P - \sigma - \sigma')}R \tag{5}$$

where σ' is given by

$$\sigma' = \frac{1}{3}\left(\frac{8S}{\rho U^2 R_0}\right)\left[\frac{1}{6}\left(\frac{8S}{\rho U^2 R_0}\right)\frac{1}{\sigma + \left(\frac{8S}{\rho U^2 R_0}\right)}\right]^{\frac{1}{2}} \tag{6}$$

Now, the minimum pressure which a nucleus experiences in flow of the type considered here is a function of the streamline offset, y, normal to the headform surface. And the bubble size at the point where the pressure reaches the minimum pressure is approximately half of the maximum bubble size, $R_{max}/2$. Thus the critical radius is given by

$$r_e = \frac{4}{3}\frac{(-C_{PM}(y) - \sigma)}{(-C_{PM}(y) - \sigma - \sigma')}\left(\frac{R_{max}}{2}\right) \tag{7}$$

Thus, only those nuclei outside r_e can cavitate. Note in equation (6) that r_e is a function of y and R_0.

It follows that the number of nuclei which will not cavitate due to the pressure perturbation surrounding a growing bubble is

$$n_i = \int_0^\infty \frac{4}{3}\pi\left[r_e^3 - \left(\frac{R_{max}}{2}\right)^3\right]N(R_0)dR_0 \tag{8}$$

Only one nucleus out of $1+n_i$ nuclei will actually cavitate. Thus, the effective nuclei number density distribution is given by

$$\frac{N(R)}{1+n_i} \tag{9}$$

where

$$n_i = \frac{1}{6}\pi R_{max}^3 \int_0^\infty N(R_0)\left[\frac{64}{27}\left(\frac{-C_{PM}(y) - \sigma}{-C_{PM}(y) - \sigma - \sigma'}\right)^3 - 1\right]dR_0 \tag{10}$$

Note that the effect of bubble interactions, n_i, is proportional to the cube of the maximum bubble size, R_{max}, which is proportional the headform scale. This means that, for a small model, bubble interactions may not be very important for the cavitation event rate. But for a large model, interactions may be very important. We also note that when $n_i \gg 1$, $1 + n_i \approx n_i$. This implies that, when the bubble interactions become large ($n_i \gg 1$), the event rate becomes independent of the nuclei concentration.

Figure 4 presents some of the typical results for a $5.08cm$ Schiebe body and a tunnel speed of $9m/s$. The individual changes in the event rate due to four separate effects are shown in the figure, namely the boundary layer flux effect, the finite size effect, the screening effect and the bubble interaction effect. The finite size effect assumes that the observer will only detect bubbles whose maximum radius is greater than $1mm$. Note that all these effects produce significant alterations in the event rate. Among the effects, the bubble screening effect causes the greatest reduction in the event rate. At high cavitation

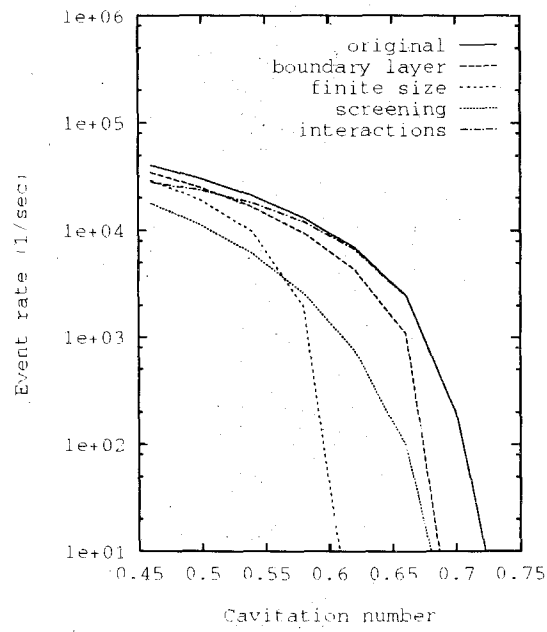

Figure 4: Typical event rates calculated using an assumed but typical nuclei distribution for flow around a $5.08cm$ Schiebe body at a velocity of $9m/s$. **Original**: Basic method not including the additional effects included in other lines. **Boundary layer**: As original but including the boundary layer flux effect. **Finite size**: As original but including only "observable" bubbles larger than $1mm$ in radius. **Screening**: As original but including the bubble screening effect. **Interactions**: As original but including the bubble interaction effect.

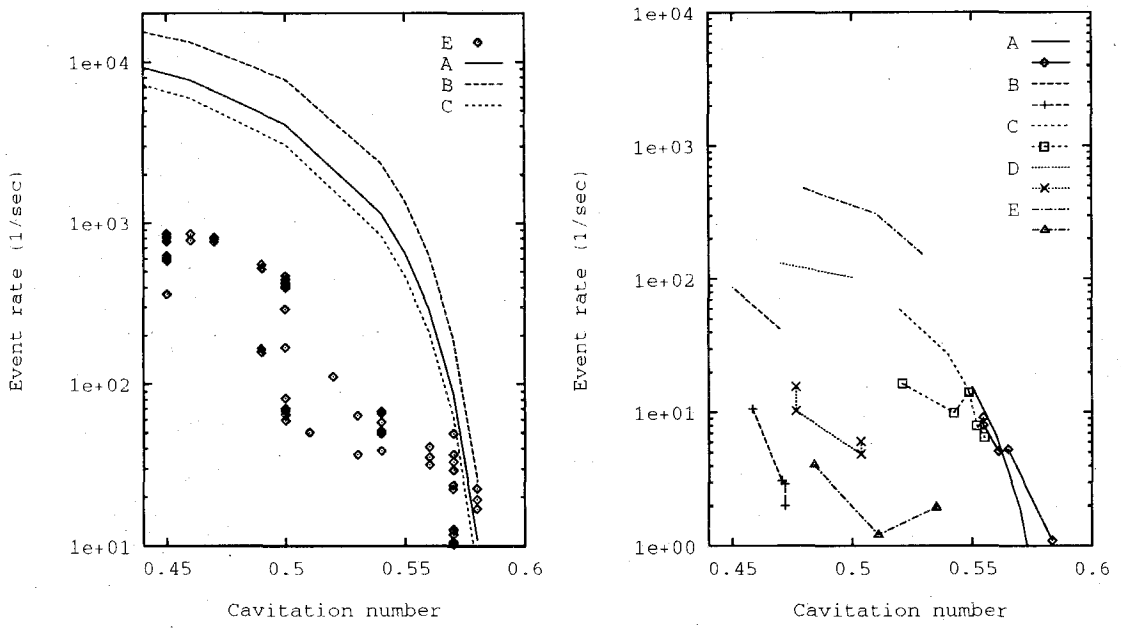

Figure 5: **Left**: A comparison of observed cavitation event rates ($\diamond$) on a $5.08cm$ Schiebe body in the LTWT at a speed of $9m/sec$ with anticipated event rates based on simultaneously measured nuclei distributions. The numerical results are plotted as (**A**): event rates calculated using the largest nuclei concentrations, (**B**): event rates calculated using intermediate nuclei concentrations, (**C**): event rates calculated using the smallest nuclei concentrations. **Right**: A comparison of observed cavitation event rates (lines with symbols) on a $5.08cm$ Schiebe body in the HSWT at various speeds and nuclei concentrations with the anticipated event rates (corresponding lines without symbol) based on simultaneously measured nuclei distributions. The data is plotted for various tunnel speeds and nuclei concentrations as follows, (**A**): $U = 8.1m/sec$, $3.6 < C < 4.3cm^{-3}$, (**B**): $U = 9.4m/sec$, $C = 0.8cm^{-3}$, (**C**): $U = 9.4m/sec$, $1.7 < C < 2.4cm^{-3}$, (**D**): $U = 12.6m/sec$, $2.0 < C < 3.0cm^{-3}$, (**E**): $U = 14.5m/sec$, $1.6 < C < 2.9cm^{-3}$.

numbers the effect of bubble/bubble interactions causes little or no reduction in the cavitation event rate. However, at low cavitation numbers, it causes significant reduction. As for the boundary layer flow rate effect, its effect is more obvious at the large cavitation numbers since the boundary layer thickness is comparable to the thickness of the low pressure region in which nuclei cavitate.

The effects of the boundary layer flow rate and of bubble screening varied slightly with flow velocity and headform scale. The effects of bubble/bubble interactions, however, varied significantly with headform size since the bubble size increases with the headform size. As the headform scale increases, the reduction of the cavitation event rate at low cavitation numbers due to bubble/bubble interactions increases with the cube of the headform radius. For the values chosen and at a cavitation number of $\sigma = 0.46$ the bubble interaction factor, n_i, is 0.9 for a headform radius of $2.5cm$. At the same cavitation number, but with a headform radius of $25cm$, the bubble/bubble interaction factor, n_i, is 900, which implies significant reduction in the cavitation event rate. Note, however, that the cavitation on the headform will transition to fully-attached cavitation long before bubble/bubble interactions reach that level.

Figure 5 presents comparisons between the experimentally measured event rates and the predictions using the simultaneously measured nuclei distributions. Note that the event rates are in rough agreement at the larger cavitation numbers but that a progressively increasing discrepancy develops as the cavitation number decreases and the event rate increases.

Finally we observe that the prediction of the cavitation inception number is inextricably connected with a detailed understanding of the event rate (see Billet and Holl [2]). In figure 6 we make a qualitative comparison between the inception number observed in the LCC experiments of Kuhn de Chizelle *et al.* [17][18] and those calculated from the model of Liu *et al.* [22] using an assumed but typical nuclei distribution function. Both the observed and calculated σ_i are based on an arbitrarily chosen critical event rate of 50 events per second. In comparing the two graphs in figure 6 we note that the scaling with size is similar while the scaling with speed is quite different probably for the reason given at the end of section 3.

5. CONCLUSIONS

The present paper describes investigations of the relationship between the cavitation nuclei distributions in water tunnels and the cavitation event rates on some axisymmetric headforms. The cavitation event rates and the nuclei populations in two water tunnels were simultaneously measured. The event rate increases with an increasing nuclei population and a decreasing cavitation number as expected. However it decreased with an increasing tunnel

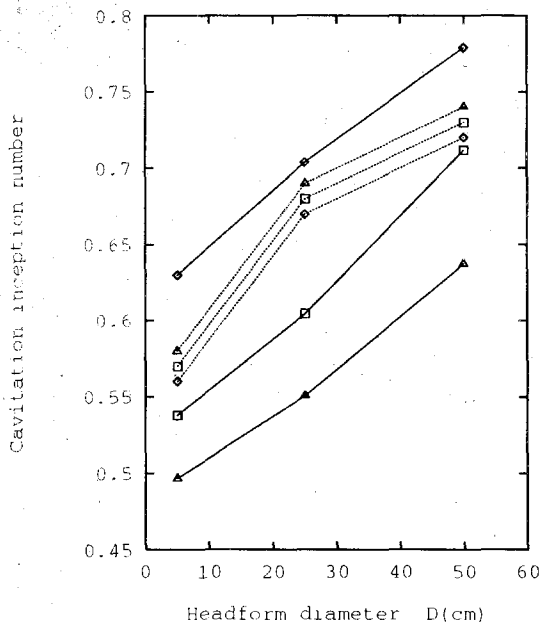

Figure 6: A comparison of cavitation inception numbers observed in the scaling experiments of Kuhn de Chizelle *et al.* [17] (dotted lines) and those predicted by the analytical model based on a critical event rate of $50s^{-1}$, an assumed but typical nuclei distribution and a minimum observable bubble radius of $1mm$ (solid lines). Data is shown for three different speeds ($9m/s = \diamond$, $11.5m/s = \square$, $15m/s = \triangle$)

speed even when the nuclei concentrations were similar. This is the inverse of what would be expected.

A simple analytical model is presented for the connection between the nuclei distribution and the event rate. The effects of the reduction in the cavitation event rate due to the complications of the reduction of volume flow rate by boundary layer, of the bubble screening near the stagnation point, of the interactions between bubbles and of a minimum observable cavitation bubble size are included. Among all these effects, bubble screening results in the largest reduction in cavitation event rate and the effect of bubble/bubble interactions becomes increasingly important with increasing body size and decreasing cavitation number. Combined, these effects give rise to a reduction in the event rate of an order of magnitude.

The scaling of the predicted cavitation event rate with body size, cavitation number and nuclei population agrees with the experimental observations. At larger cavitation numbers, the predicted cavitation event rates quantitatively agree with experimental observations in the Low Turbulence Water Tunnel and the High Speed Water Tunnel. However, two outstanding issues still remain. First the observed event rates at lower cavitation numbers are about an order in magnitude smaller than one would predict based on the actual nuclei distributions. This may be due to the fact that only a fraction of the observed nuclei actually cavitate or it may be due to some other effect which is not included in the model. More study is needed to confirm this. Second, the changes with tunnel velocity cannot be fully explained at present.

When the model for the event rates is used with some chosen criterion to predict the cavitation inception number, the results are consistent with those observed experimentally in so far as the trend with headform size is concerned. The trend with velocity is, of course, at odds with the experiments because of the discrepancy in the event rate discussed above.

ACKNOWLEDGEMENTS

The authors would like to thank Pavel Svitek, Fabrizio D'Auria, Garrett Reisman, Yi-chun Wang and Elizabeth McKenney for help with the experiments in the High Speed Water Tunnel. This work was supported by the Office of Naval Research under contract number N-00014-91-K-1295.

References

[1] Arndt, R. E. A. and Keller, A. P., 1976, "Free gas content effects on cavitation inception and noise in a free shear flow, " *Proc. IAHR Conf. on Two Phase Flow and Cavitation in Power Generation Systems*, Grenoble, France, pp. 3–16.

[2] Billet, M. L. and Holl, J. W., 1979, "Scale effects on various types of limited cavitation," *ASME Int. Symp. on Cavitation Inception*, pp. 11-24.

[3] Billet, M. L., 1985, "Cavitation nuclei measurement – a review," *ASME Cavitation and Multiphase Flow Forum Booklet*, pp. 31-38.

[4] Blake, F. G., 1949, "The onset of cavitation in liquids: I," *Acoustics Res. Lab., Harvard Univ., Tech. Memo.*, No. 12.

[5] Brennen, C. E., 1994, "Cavitation and bubble dynamics", Oxford University Press.

[6] Cartmill, J. W. and Su, M. Y, 1993, "Bubble size distribution under saltwater and freshwater breaking waves," *Dynamics of Atmospheres and Oceans*, vol. 20, pp. 25-31.

[7] Ceccio, S. L. and Brennen, C. E., 1992, "Observations of the dynamics and acoustics of traveling bubble cavitation," *J. Fluid Mech.*, Vol. 233, pp. 633-660

[8] Feldberg, L. A. and Shlemenson, K. T., 1971, "The holographic study of cavitation nuclei," *Proc. IUTAM Symp. Non-steady Flow of Water at High Speed*, Leningrad, USSR, pp. 239–42,

[9] Gates, E. M. and Acosta, A. J., 1978, "Some effects of several free-stream factors on cavitation inception on axisymmetric bodies," *Proc. 12th ONR Symp. on Naval Hydrodynamics*, pp. 86–108.

[10] Gates, E. M. and Bacon, J., 1978, "A note on the determination of cavitation nuclei distributions by holography," *J. Ship Research*, Vol. 22(1), pp. 29–31

[11] Gindroz, B. and Billet, M. L., 1994, "Nuclei and propeller cavitation inception," *Proc. ASME Symp. on Cavitation and Gas-Liquid Flow in Fluid Machinery and Devices*, ASME. FED-Vol. 190, pp. 251-269.

[12] Johnson, V. E. and Hsieh, T., 1966, "The Influence of Gas Nuclei on Cavitation Inception," *Proc. 6th Symp. on Naval Hydrodynamics, Washington, D.C.*, National Academy Press.

[13] Keller, A. P., 1972, "The influence of the cavitation nucleus spectrum on cavitation inception, investigated with a scattered light counting method," *ASME J. Basic Eng.*, pp. 917–925.

[14] Keller, A. P., 1974, "Investigations concerning scale effects of the inception of cavitation," *Proc. I. Mech. E. Conf. on Cavitation*, pp. 109–117.

[15] Keller, A. P. and Weitendorf, E. A., 1976, "Influence of undissolved air content on cavitation phenomena at the propeller blades and on induced hull pressure amplitudes," *Proc. IAHR Symp. on Two Phase Flow and Cavitation in Power Generation Systems*, pp. 65–76.

[16] Kuiper, G., 1978, "Scale effects on propeller cavitation inception," *Proc. 12th ONR Symp. on Naval Hydrodynamics*, pp. 400–429.

[17] Kuhn de Chizelle, Y., Ceccio, S. L., Brennen C. E. and Shen, Y., 1992, "Cavitation scaling experiments with headforms: bubble dynamics," *Proc. 2nd Int. Symp. on Propeller and Cavitation*, Hangzhou, China.

[18] Kuhn de Chizelle, Y., Ceccio, S. L., Brennen C. E. and Shen, Y., 1992, "Cavitation scaling experiments with headforms: bubble acoustics," *Proc. 19th Symp. on Naval Hydrodynamics*, Seoul, Korea, pp. 72–84.

[19] Le Goff, J. P. and Lecoffre, Y., 1983, "Nuclei and cavitation", *Proc. 14th Symp. on Naval Hydrodynamics*, National Academy Press, pp. 215–242.

[20] Li, C. Y. and Ceccio, S. L., 1994, "Observations of the interactions of cavitation bubbles with attached cavities," *Proc. ASME Symp. on Cavitation and Gas-Liquid Flow in Fluid Machinery and Devices*, ASME. FED-Vol. 190, pp. 283–290.

[21] Liu, Z., Sato, K. and Brennen, C. E., 1993, "Cavitation nuclei population dynamics in a water tunnel," *ASME Cavitation and Multiphase Flow Forum*, FED-Vol. 153, pp. 119–125.

[22] Liu, Z., Kuhn de Chizelle, Y. and Brennen, C. E., 1993, "Cavitation event rates and nuclei distributions," *Proc. ASME Symp. on Cavitation Inception*, FED-Vol. 177, pp. 13–24.

[23] Liu, Z. and Brennen, C. E., 1994, "The relation between the nuclei population and the cavitation event rate for cavitation on a Schiebe body," *Proc. ASME Symp. on Cavitation and Gas Liquid Flows in Fluid Machinery*, pp. 261–266.

[24] Meyer, R. S., Billet, M. L. and Holl, J. W., 1992, "Freestream Nuclei and Traveling Bubble Cavitation," *ASME J. Fluids Eng.*, Vol. 114, pp. 672-679.

[25] Oldenziel, D. M., 1982, "A new instrument in cavitation research: the cavitation susceptibility meter," *ASME J. Fluids Eng.*, Vol. 104, pp. 136–142.

[26] Parkin, B. R., 1952, "Scale effects in cavitating flow," *Ph.D. Thesis, Calif. Inst. of Tech.*.

[27] Peterson, F. B., 1972, "Hydrodynamic cavitation and some considerations of the influence of free gas content," *Proc. 9th Symp. on Naval Hydrodynamics*, Paris, 1972.

[28] Peterson, F. B., Danel, F., Keller, A. and Lecoffe, Y., 1975, "Determination of bubble and particulate spectra and number density in a water tunnel with three optical techniques," *Proc. 14th ITTC*, volume 2, Ottawa, pp. 27–52.

[29] Plesset, M. S., 1949, "The dynamics of cavitation bubbles," *ASME J. Appl. Mech.*, Vol. 16, pp. 228-231.

[30] Saffman, M., Buchhave, P. and Tanger, H., 1984, "Simultaneous measurements of size, concentration and velocity of spherical particles by a laser Doppler method," *Proc. 2nd Int. Symp. on Applications of Laser Anemometry to Fluid Mechanics, Lisbon.*

[31] Schiebe, F. R., 1972, "Measurement of the cavitation susceptibility of water using standard bodies," *Rep. 118*, St. Anthony Falls Hydraulic Lab, University of Minnesota.

[32] Tanger, H. and Weitendorf, E. A., 1992, "Applicability tests for the phase Doppler anemometer for cavitation nuclei measurements," *ASME J. Fluids Eng.*, Vol. 114, pp. 443–449.